

## Communications

### Structure of Anodic Oxide Coatings on Aluminum \*\*

By Rüdiger Kniep,\* Peter Lamparter and Siegfried Steeb

Porous surface coatings on aluminum are produced by anodic oxidation in acid electrolytes.<sup>[1]</sup> Pore sizes (10–250 nm) as well as pore densities ( $10^{12}$ – $10^{15}$  m<sup>-2</sup>) are mainly controlled by the anodizing voltage; the thickness of the layers may reach more than 100  $\mu$ m and is determined by the amount of charge transferred. The remarkably uniform array of the pores in the centers of the almost hexagonally shaped cells makes the films of interest for application in the field of synthetic membranes and as supports for active materials.<sup>[2, 3]</sup> Furthermore, the coatings are widely used as protective layers which can also be colored by impregnation of the pores with organic dyes or by precipitation of inorganic pigments in the pores.<sup>[4, 5]</sup> After coloring, the pores are closed by treatment with water or steam. This “sealing” process causes the formation of gelatinous boehmite and amorphous oxide hydroxide by reaction of the pore wall material with water.<sup>[6]</sup>

The structure of the (amorphous) porous coatings is not clear at present. It is assumed that they are structurally related to the non-porous “barrier-layer” (in direct contact with the metal; thickness 0.1–0.2  $\mu$ m) which consists of almost pure Al<sub>2</sub>O<sub>3</sub> and contains the  $\eta$ - and  $\gamma$ -phases of alumina (spinel-type structures). This assumption is supported by the primary products of crystallization which are formed by thermal treatment of the porous coatings and which were identified as the  $\gamma$ - and  $\gamma'$ -phases of alumina.<sup>[7]</sup> A recent IR-investigation of dried porous layers<sup>[8]</sup> is consistent with coordination numbers of four and six (tetrahedral and octahedral) for the aluminum atoms.

In the present work freshly prepared porous coatings were investigated with X-ray and neutron diffraction methods. The aluminum atoms were found mostly to be surrounded tetrahedrally by four oxygen atoms. The close similarities of the radial distribution function (RDF) of the porous layers to that of vitreous silica suggest that the same structural model should be applied for both materials.

Samples for the diffraction experiments were prepared by anodic oxidation of aluminum foils applying the following parameters: bath temperature 12 °C; natural bath convection; current 1.5 A/dm<sup>2</sup>; voltage 15 V; Al<sup>3+</sup> content in the bath 5.2 g/l; H<sub>2</sub>SO<sub>4</sub>(total) 200 g/l; H<sub>2</sub>SO<sub>4</sub>(free) 172 g/l. The layers were removed from the metal by treatment with Br<sub>2</sub>/MeOH mixtures. The chemical composition of a large number of samples was determined using XFA (Al and S), IC

(SO<sub>4</sub><sup>2-</sup>), EDX (Al and S) and TG (H<sub>2</sub>O) and yielded a mean brutto-formula of (5 Al<sub>2</sub>O<sub>3</sub> · SO<sub>3</sub> · 0.66 H<sub>2</sub>O) · 1.33 H<sub>2</sub>O with deviations less than one wt-% for the distinct components. The amount of water given inside the brackets of the formula is regarded as the water of constitution (OH-groups) which is released only at temperatures above 470 °C; the amount of water given outside the brackets is regarded as H<sub>2</sub>O-molecules (structural water and/or adsorbed water at the pore walls) which is already released between 80 °C and 250 °C.

Figure 1 (a) shows the X-ray structure factors  $S^X(Q)$  from angular dispersive X-ray diffraction (ADX) and from en-

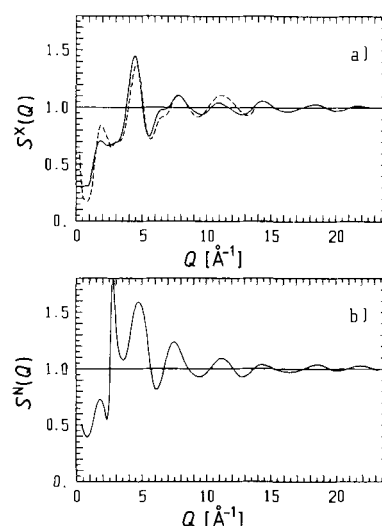


Fig. 1. Amorphous anodic oxide coatings on aluminum. Structure factors  $S(Q)$ , calculated from a) ADXD (---), EDXD (—) and b) Neutron diffraction.  $S(Q) = (I(Q) - \langle b^2 \rangle - \langle b \rangle^2) / \langle b \rangle^2$  where  $I(Q)$  = coherently scattered intensity per atom;  $\langle b^2 \rangle$  = mean squared scattering length per atom;  $\langle b \rangle$  = mean scattering length (with X-rays depending on  $Q$ ).

ergy dispersive X-ray diffraction (EDXD). Both curves have the same overall shape without sharp reflexes, giving evidence that the anodic oxide coating material is amorphous. In the region of the first peak near  $Q = 2.8 \text{ \AA}^{-1}$  the EDXD reflects lower resolution, whereas the high  $Q$ -tail of the ADXD curve near  $Q = 12 \text{ \AA}^{-1}$  we judge to be less reliable. The observation of extended oscillations up to  $Q = 23.5 \text{ \AA}^{-1}$  demonstrates the power of the EDXD method. The same high- $Q$  oscillations are observed with the neutron structure factor  $S^N(Q)$  in Figure 1 (b). At smaller  $Q$ , however,  $S^N$  is different from  $S^X$  where the most drastic difference is the appearance of a large sharp peak in  $S^N$  at  $Q = 2.8 \text{ \AA}^{-1}$  which in  $S^X$  shows up only as a small hump. The reduced pair correlation functions  $G(R)$ , calculated from the structure factors by Fourier-transformation are shown in Figure 2. The restriction of the range, up to only  $R = 6 \text{ \AA}$ , is justified by the abrupt loss of any correlations in the X-ray curves  $G^X(R)$  beyond  $R = 4.6 \text{ \AA}$ . This signifies that the structural units built up by the aluminum and oxygen atoms in the amorphous phase have a very small extension of maximum of about 5  $\text{\AA}$ . On the other hand, the neutron curve  $G^N(R)$

[\*] Prof. Dr. R. Kniep  
Eduard-Zintl-Institut  
Technische Hochschule Darmstadt  
Hochschulstraße 10  
D-6100 Darmstadt (FRG)

Dr. P. Lamparter, Prof. Dr. S. Steeb  
Max-Planck-Institut für Metallforschung  
Institut für Werkstoffwissenschaft  
Seestraße 92  
D-7000 Stuttgart 1 (FRG)

[\*\*] This work was supported by the Fonds der Chemischen Industrie and by the Henkel KGaA

exhibits very extended oscillations up to  $R = 20 \text{ \AA}$ . Obviously, these extended correlations involve hydrogen atoms which are practically invisible to X-rays. Details of the hydrogen scattering will not be under consideration in this study.

For the identification of the peaks in the  $G(R)$  functions in Figure 2 the weighting factors of the ten partial correlation

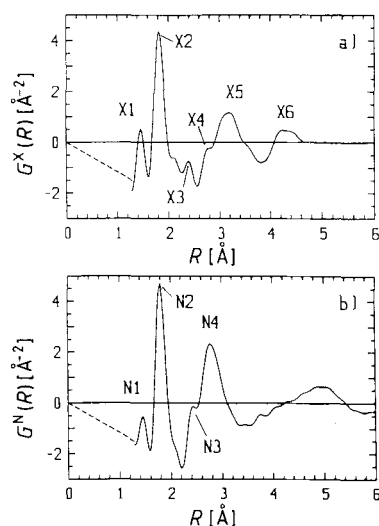


Fig. 2. Amorphous anodic oxide coatings on aluminum. Correlation functions  $G(R)$ , calculated by Fourier transformation from the structure factors  $S(Q)$  in Fig. 1 (a): EDXD; (b): Neutron diffraction;  $G(R) = \frac{2}{\pi} \int_0^\infty Q[S(Q) - 1] \sin QR dQ$  where  $G(R) = 4\pi R [\rho(R) - \rho_0]$ ;  $\rho(R)$  = pair density distribution function;  $\rho_0$  = mean number density;  $R$  = distance in real space.

functions  $G_{ij}(R)$ , ( $i, j = \text{Al, O, S, H}$ ), which contribute to  $G(R)$  are listed in Table 1.

The most important information on the short range order in the amorphous coatings is extracted from the main peak of  $G(R)$  at  $R = 1.80\text{--}1.82 \text{ \AA}$  (X2 and N2 in Fig. 2) which represents the Al-O nearest neighbors. The almost equal  $W_{\text{AlO}}$  for X-rays and neutrons (Tab. 1) are in accordance

Tab. 1. Weighting factors  $W_{ij}$  of the partial correlation functions  $G_{ij}(R)$  ( $i, j = \text{Al, O, S, H}$ ). Upper numbers for X-rays; lower numbers for neutrons.  $G(R) = \sum_{ij} W_{ij} G_{ij}(R)$ , where  $W_{ij} = \delta c_i c_j b_i b_j / \langle b \rangle^2$ ;  $c_i$  = atomic concentration;  $\delta = 1$  when  $i = j$ ,  $\delta = 2$  when  $i \neq j$ .

	Al	O	S	H
Al	0.176 0.062	—	—	—
O	0.433 0.418	0.266 0.703	—	—
S	0.043 0.010	0.053 0.035	0.003 0.000	—
H	0.011 -0.054	0.013 -0.181	0.001 -0.005	0.000 0.012

with the equal amplitudes of the corresponding peaks. From the area under the peaks in the radial distribution functions ( $\text{RDF}^{\text{X,N}}(R) = 4\pi R^2 \rho^{\text{X,N}}(R) = RG^{\text{X,N}}(R) + 4\pi R^2 \rho_0$ ) the coordination number of oxygen atoms around Al is obtained

as  $4 \leq Z_{\text{AlO}} \leq 5$  depending on the choice of  $\rho_0$ , i.e., the macroscopic density  $D$ . According to this method the aluminum atoms are mostly surrounded tetrahedrally by four oxygen atoms.  $Z_{\text{AlO}} = 4$  is obtained using the macroscopic density  $D = 2.75 \text{ g cm}^{-3}$  as determined by the Archimedeian method. This experimental  $D$ -value might be somewhat too small, due to amounts of adsorbed air in the pores of the films. An estimated extrapolation of the densities of amorphous  $\text{SiO}_2 \cdot \text{Al}_2\text{O}_3$  materials ( $Z = 4.3\text{--}4.6$ )<sup>[9]</sup> yields  $D = 3.3 \text{ g cm}^{-3}$  for pure amorphous  $\text{Al}_2\text{O}_3$ . The Al-O distance at  $1.81 \text{ \AA}$  in the amorphous porous coatings (Fig. 2) is smaller than the octahedral Al(6)-O distances observed in  $\alpha\text{-Al}_2\text{O}_3$  ( $1.86\text{--}1.97 \text{ \AA}$ <sup>[10]</sup>) and in boehmite ( $1.88\text{--}1.94 \text{ \AA}$ <sup>[11]</sup>) and is somewhat larger than the tetrahedral bond lengths Al(4)-O/OH ( $1.73\text{--}1.78 \text{ \AA}$ ) in the isolated dimeric anion  $[\text{Al}_2\text{O}(\text{OH})_6]^\ominus$ .<sup>[12]</sup>

According to the significant amount of sulfate in the porous anodic oxide coatings, the peaks X1 (N1) and X3 (N3) in Figure 2 can be attributed to  $\text{SO}_4$ -tetrahedra. The peaks X1 (N1) at  $R = 1.45 \text{ \AA}$  correspond to S-O bonds ( $1.47\text{--}1.50 \text{ \AA}$ ) in  $\text{SO}_4^{2-}$  groups. Its height scales well with the respective  $W_{\text{SO}}$  in Table 1. The O-O distance along an edge of a  $\text{SO}_4$ -tetrahedron is expected at  $R_{\text{O-O}} = \sqrt{8/3} R_{\text{S-O}} = 2.38 \text{ \AA}$ , and shows up at X3 (N3) in the correlation functions. In accordance with  $W_{\text{O-O}}$  the peak appears higher with neutrons.

In the following we discuss the  $G(R)$  curves in Figure 2 on the basis of the structural model for the short range order in the amorphous anodic coatings as presented in Figure 3:

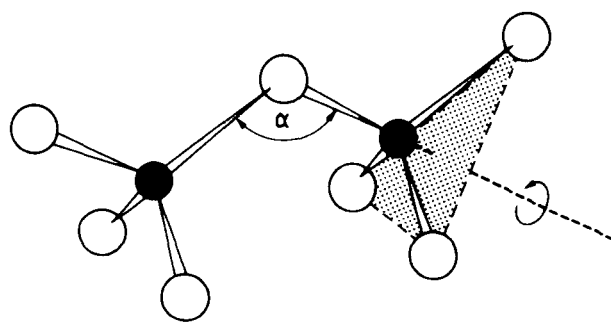


Fig. 3. Short range order in amorphous anodic oxide coatings on aluminum.

Two  $\text{AlO}_4$  tetrahedra share a common oxygen corner; the irregular three dimensional structure is then controlled by the possible variations of the angle  $\alpha$ , (Al-O-Al), as well as by the conformational statistics resulting from "free" rotation of the tetrahedra around their O-Al-axes. Preferred tetrahedral coordination of aluminum (Al-O  $1.81 \text{ \AA}$ ) has already been deduced from the peaks X2 (N2) in Figure 2. The distance between two O-atoms along an edge of a tetrahedron is expected for the case of perfect tetrahedra at  $R_{\text{O-O}} = \sqrt{8/3} R_{\text{Al-O}} = 2.95 \text{ \AA}$ . We attribute the peaks X4 (N4) at  $2.80 \text{ \AA}$  to this O-O distance which, according to Table 1, appears stronger with neutrons. The average O-O distance along an edge of a tetrahedron in the structure of  $\text{K}_2 [\text{Al}_2\text{O}(\text{OH})_6]$  is  $2.86 \text{ \AA}$ .<sup>[12]</sup> With X-rays, a peak X5 appears at larger  $R = 3.20 \text{ \AA}$  which reflects Al...Al distances resulting from

corner-sharing  $\text{AlO}_4$  tetrahedra; according to Table 1 its contribution is much weaker with neutrons. The angle  $\text{Al}(4)\text{-O}(2)\text{-Al}(4)$  of  $132^\circ$  in the isolated dimeric tetrahedral anion  $[\text{Al}_2\text{O}(\text{OH})_6]^\ominus$  [12] corresponds with a respective distance  $\text{Al}\cdots\text{Al}$  of  $3.18 \text{ \AA}$ . Larger Al-O as well as O-O distances give rise to the peak X6 around  $4.3 \text{ \AA}$ . Whether the fine structure in  $G^N(R)$  in this region is real or is caused by Fourier-ripples cannot be decided presently. It is expected that the broad peaks X5 and X6 are also contributed by non-bonding interactions which reflect the partial substitution of aluminum by sulfur in the amorphous structure.

It should be noted that the short range order in amorphous anodic oxide coatings on aluminum shows close similarities to the short range order reported for vitreous silica. [13-17]

Standardization of the chemical composition  $(5 \text{ Al}_2\text{O}_3 \cdot \text{SO}_3 \cdot 0.66 \text{ H}_2\text{O}) \cdot 1.33 \text{ H}_2\text{O}$  of the porous anodic oxide coatings to a structural formula  $(\text{A})^n[\text{X}_{n/2}]$ , which in the case of  $n = 4$  represents the idealized structure of vitreous silica, leads to  $(\text{Al}_{0.91} \text{S}_{0.09})^{[3,39]} [\text{O}_{3.15/2} (\text{OH})_{0.24/2}]$  with the water outside the brackets of the oxide formula not taken into consideration. The coordination number of oxygen atoms around aluminum ( $4 \leq Z_{\text{AlO}} \leq 5$ ) which is derived from the  $\text{RDF}^{\text{X,N}}$  shows that the oxygen and hydroxyl-groups are not exclusively bound to only two adjacent cations, an observation which is also valid for the structure of vitreous silica. [17]

A final remark should be made concerning the morphology of the almost hexagonally shaped cells (each containing a pore) which has been discussed as an indication of crystallinity of the anodic oxide layers. The isotropic (circular) growth of cells starts at nuclei which are homogeneously distributed over the surface of the aluminum metal. In the course of growth the cells come into contact and develop a homogeneous nearly hexagonal array of cell boundaries which covers the complete coating surface. A pore size near  $150 \text{ \AA}$  and a distance between the pores of about  $370 \text{ \AA}$  was determined from small angle neutron scattering (SANS) [18] studies on a deuterated sample which was prepared under the same anodizing conditions as applied for the materials for the structural investigations.

### Experimental

The X-ray diffraction experiments were performed in transmission mode using two different techniques: Angular dispersive X-ray diffraction (ADX) with a conventional D500-Siemens diffractometer and energy dispersive X-ray diffraction (EDXD) with a laboratory-built set up. [19] The sample material was powdered and filled into a flat container with Kapton-foil windows mounted in a vacuum chamber. With ADXD (EDXD) the scattering could be recorded up to the scattering vectors  $Q = 13.5 \text{ \AA}^{-1}$  ( $23.5 \text{ \AA}^{-1}$ ), where  $Q = 4\pi \sin \theta / \lambda$ . Correction methods and normalization to absolute units were applied as described elsewhere. [20, 21] The structure factors  $S(Q)$  were calculated according to the Faber-Ziman definition. [22]

The neutron diffraction experiments were performed at the Institute-Laue-Langevin using the instrument D4B up to  $Q = 23.3 \text{ \AA}^{-1}$ . The evaluation of the structure factor  $S(Q)$  was done essentially as reported elsewhere. [23] However, in the present case the incoherent scattering contribution of the hydrogen in the sample had to be corrected for. This was achieved by fitting a smooth function through the absorption corrected intensity curve in such a way that after the subtraction of the smooth H-contribution the resulting structure factor oscillated properly around one. This smooth function agreed very well with a previously reported [24] hydrogen scattering function. Furthermore, from its intensity an H-content of  $10.6 \text{ at-\%}$  was calculated which corresponds well to the analytical value of  $11.4 \text{ at-\%}$ .

Received April 13, 1989

- [1] V. F. Henley: *Anodic Oxidation of Aluminum and Its Alloys*, Pergamon Press, New York 1982.
- [2] R. C. Furneaux, W. R. Rigby, A. P. Davidson, *Nature London* 337 (1989) 147.
- [3] D. L. Cocke, D. E. Johnson, R. P. Merrill, *Catal. Rev. Sci. Eng.* 26 (1984) 163.
- [4] S. Tajima, *Adv. Corr. Sci. Technol.* 1 (1970) 227.
- [5] K. Wefers, P. F. Wallace, *Aluminium (Düsseldorf)* 52 (1976) 485.
- [6] K. Wefers, *Aluminium (Düsseldorf)* 49 (1973) 622.
- [7] A. Roth, *Z. Anorg. Allg. Chem.* 244 (1940) 48.
- [8] A. B. Kiss, E. Szontagh, G. Kresztury, *Aluminium (Düsseldorf)* 61 (1985) 821.
- [9] H. Morikawa, S. Miwa, M. Miyake, F. Marumo, T. Sata, *J. Am. Ceram. Soc.* 65 (1982) 78.
- [10] R. E. Newnham, Y. M. de Haan, *Z. Krist.* 117 (1962) 235.
- [11] R. J. Hill, *Clays Clay Miner.* 29 (1981) 435. C. E. Corbato, R. T. Tettendorf, G. C. Christoph, *ibid* 33 (1985) 71.
- [12] G. Johansson, *Acta Chem. Scand.* 20 (1966) 505.
- [13] R. J. Bell, P. Dean, *Philos. Mag.* 25 (1972) 1381.
- [14] K. Zickert, H. Steil, C. Geik, G. Herms, G. Becherer, *Krist. Tech* 14 (1979) 1147.
- [15] R. L. Mozzi, B. E. Warren, *J. Appl. Cryst.* 2 (1969) 164.
- [16] B. E. Warren, H. Krutter, O. Morningstar, *J. Am. Ceram. Soc.* 19 (1936) 202.
- [17] A. Felz: *Amorphe und glasartige anorganische Festkörper*, Akademie-Verlag, Berlin 1983.
- [18] R. Kniep, P. Lamparter, S. Steeb, unpublished.
- [19] R. Utz: *Diploma Thesis*, University Stuttgart, 1987.
- [20] P. Lamparter, A. Habenschuss, A. H. Narten, *J. Non-Cryst. Solids* 86 (1986) 109.
- [21] T. Egami, *J. Appl. Phys.* 50 (1979) 1564.
- [22] T. E. Faber, J. M. Ziman, *Philos. Mag.* 11 (1965) 153.
- [23] P. Lamparter, W. Sperl, S. Steeb, J. Bléry, *Z. Naturforsch.* 37a (1982) 1223.
- [24] P. Chieux, R. de Kouchkovski, B. Boucher, *J. Phys. F* 14 (1984) 2239.

### Superconductivity at 7.5 K and Ambient Pressure in Polycrystalline Pressed Samples of $\beta_p\text{-(BEDT-TTF)}_2\text{I}_3^{**}$

By Dieter Schweitzer\*, Emil Gogu, Hans Grimm, Siegfried Kahlich and Heimo J. Keller

Recently, bulk superconductivity at ambient pressure in polycrystalline pressed samples of an organic metal— $\alpha\text{-(BEDT-TTF)}_2\text{I}_3$ —was observed. [1] This is a remarkable fact because this finding shows that organic superconductors can in principle be used for the production of electronic devices, such as squids, and might even be suitable for the preparation of superconducting cables similar to the high temperature superconductors of the copper oxides.

The polycrystalline pressed samples of  $\alpha\text{-(BEDT-TTF)}_2\text{I}_3$  were prepared from pulverized single crystals of  $\alpha\text{-(BEDT-TTF)}_2\text{I}_3$  and the pressed samples had to be annealed at  $75^\circ\text{C}$

- [\*] Prof. Dr. D. Schweitzer  
Physikalisches Institut der Universität Stuttgart  
Pfaffenwaldring 57, D-7000 Stuttgart 80 (FRG)  
Dipl. Phys. E. Gogu, Dr. H. Grimm, Dipl. Phys. S. Kahlich  
Max Planck Institut für Medizinische Forschung, AG Molekülkristalle  
Heidelberg (FRG)  
Prof. Dr. H. J. Keller  
Anorganisch Chemisches Institut der Universität Heidelberg  
Heidelberg (FRG)

[\*\*] We gratefully acknowledge financial support of this work by the Deutsche Forschungsgemeinschaft.